Molecular Biology of the Cell
Vol. 12, 1353–1365, May 2001

Dynamics of Immature Secretory Granules: Role of Cytoskeletal Elements during Transport, Cortical Restriction, and F-Actin-dependent Tethering

Rüdiger Rudolf,* Thorsten Salm,* Amin Rustom, and Hans-Hermann Gerdes†

Department of Neurobiology, Interdisciplinary Center for Neuroscience, University of Heidelberg, Im Neuenheimer Feld 364, D-69120 Heidelberg, Germany

Submitted June 27, 2000; Revised January 3, 2001; Accepted February 15, 2001
Monitoring Editor: Randy W. Schekman

Secretory granules store neuropeptides and hormones and exhibit regulated exocytosis upon appropriate cellular stimulation. They are generated in the *trans*-Golgi network as immature secretory granules, short-lived vesicular intermediates, which undergo a complex and poorly understood maturation process. Due to their short half-life and low abundance, real-time studies of immature secretory granules have not been previously possible. We describe here a pulse/chase-like system based on the expression of a human chromogranin B-GFP fusion protein in neuroendocrine PC12 cells, which permits direct visualization of the budding of immature secretory granules and their dynamics during maturation. Live cell imaging revealed that newly formed immature secretory granules are transported in a direct and microtubule-dependent manner within a few seconds to the cell periphery. Our data suggest that the cooperative action of microtubules and actin filaments restricts immature secretory granules to the F-actin-rich cell cortex, where they move randomly and mature completely within a few hours. During this maturation period, secretory granules segregate into pools of different motility. In a late phase of maturation, 60% of secretory granules were found to be immobile and about half of these underwent F-actin-dependent tethering.

INTRODUCTION

The secretory granule (SG) is the hormone- and neuropeptide-containing storage compartment of neuroendocrine cells and undergoes Ca^{2+}-dependent, regulated exocytosis to release its content. SGs are formed at the *trans*-Golgi network (TGN) as short-lived vesicular intermediates termed immature secretory granules (ISGs) (Tooze *et al.*, 1991). ISGs undergo a complex and poorly understood maturation process resulting in mature SGs (MSGs), which are primed and docked presumably in proximity to the plasma membrane (PM) (Robinson and Martin, 1998).

To date, the maturation process of ISGs has been studied biochemically by exploiting radioactive pulse/chase-labeling in combination with gradient analysis (Tooze *et al.*, 1991). In the rat pheochromocytoma cell line (PC12) it was found that upon maturation the buoyant density of ISGs increases with a $t_{1/2}$ of 45 min, reaching a plateau at 75 min of chase (Tooze *et al.*, 1991). Furthermore, electron microscopic studies showed that the dense core of MSGs is larger in diameter than that of ISGs (Tooze *et al.*, 1991). Based on these findings homotypic fusion of three to five ISGs was proposed (Tooze *et al.*, 1991) and supported by the use of an in vitro assay (Urbé *et al.*, 1998). Furthermore, several lines of evidence suggest that excess of membranes and missorted proteins such as the ubiquitously expressed TGN/endosomal membrane protease furin are removed from maturing ISGs by budding of clathrin-coated ISG-derived vesicles (Dittie *et al.*, 1996, 1997; Klumperman *et al.*, 1998).

Although the biochemical studies provide some insights as to which molecules participate in the maturation process, they do not address dynamics and subcellular localization of maturing SGs. Furthermore, it is not clear to what extent the vesicular maturation steps, which so far have been mainly studied in vitro (Urbé *et al.*, 1998), occur in living cells. To address these questions, live cell imaging with the use of green fluorescent protein (GFP) fusion proteins provides a valuable tool. To date, several studies have used such pro-

* These authors contributed equally to this work.
† Corresponding author. E-mail address: hhgerdes@sun0.urz.uni-heidelberg.de.

Abbreviations used: bFur, bovine furin; EGFP, enhanced GFP; GFP, green fluorescent protein; hCgB, human chromogranin B; ISG, immature secretory granule; MSG, mature secretory granule; PM, plasma membrane; SG, secretory granule; TGN, *trans*-Golgi network.

© 2001 by The American Society for Cell Biology

teins to analyze different aspects of SG dynamics such as transport in neurites (Kaether *et al*., 1997; Lochner *et al*., 1998) or exocytosis (Lang *et al*., 1997, 2000; Pouli *et al*., 1998; Han *et al*., 1999). Notably, in all these cases the GFP-based fluorescence video microscopy of live cells was carried out under steady-state conditions where nearly all fluorescent structures represent MSGs. Because ISGs are indistinguishable from MSGs by light microscopy and represent only a small minority, imaging of ISGs was not accessible. Thus, these studies led to insights into traffic of MSGs but not of ISGs.

To address specifically the dynamics of the short-lived ISGs, we made use of the fusion protein human chromogranin B (hCgB)-GFP(S65T). In contrast to enhanced GFP (EGFP), the folding of the GFP(S65T) mutant to its fluorescent form is efficient at lower temperature only but not at 37°C (Kaether and Gerdes, 1995; Patterson *et al*., 1997). Upon application of a 20°C secretion block, which inhibits biogenesis of post-TGN vesicles, the temperature sensitivity of the GFP(S65T) mutant led to a specific illumination of the TGN in hCgB-GFP(S65T) transfected HeLa cells (Kaether and Gerdes, 1995). Reversal of the temperature block permitted the visualization of biogenesis and transport of constitutive vesicles in cells lacking a regulated pathway of protein secretion (Kaether and Gerdes, 1995). We here express the same fusion protein in the neuroendocrine cell line PC12 to specifically generate fluorescent ISGs in a pulse/chase-like manner and to monitor them during their maturation. We show that shortly after synthesis at the TGN, ISGs are quickly transported in a microtubule-dependent manner into the F-actin-rich cortex underneath the PM. During their maturation, ISGs are restricted to the cortical region. Segregation of SGs into distinct pools is found to occur during the maturation period.

MATERIALS AND METHODS

Chemicals, Antibodies, and Expression Vectors

Nocodazole, phalloidin-TRITC, and phalloidin-FITC were purchased from Sigma Chemical (St. Louis, MO) and latrunculin-B from Calbiochem (La Jolla, CA). Monoclonal antibody against rat-TGN38 was kindly provided by Dr. Banting (University of Bristol, Bristol, United Kingdom (Luzio *et al*., 1990). Polyclonal antibody against bovine furin (bFur) (KL92/10) was kindly provided by Dr. Garten (University of Marburg, Marburg, Germany). Polyclonal rabbit anti-GFP antiserum D2 is described in Kaether *et al.* (1997). Monoclonal anti-α-tubulin antibody (clone DM1A) was purchased from Sigma Chemical and monoclonal anti-rat Thy1.1 antibody (clone OX-7) from PharMingen (San Diego, CA). Secondary goat anti-mouse antibody conjugated to Rhodamine-Red-X was purchased from Jackson ImmunoResearch (West Grove, PA).

Expression construct pcDNA3/hCgB-EGFP was generated by restriction of pCDM8/hCgB-EGFP (Kaether *et al*., 1997) with *Hin*dIII and *Eco*RI and ligation of the obtained hCgB-EGFP cDNA fragment into pcDNA3 expression vector (Invitrogen, San Diego, CA) opened with the corresponding restriction enzymes. The expression construct pCDM8/hCgB-GFP(S65T) is described in Kaether and Gerdes (1995), pcDNA3/PTS1-GFP was kindly provided by Dr. Just (University of Heidelberg, Heidelberg, Germany; Huber *et al*., 1997), and pcDNA3/bFur was kindly provided by Dr. Garten (University of Marburg).

Cell Culture and Transfection

PC12 cells (rat pheochromocytoma cells, clone 251; Heumann *et al*., 1983) were grown in DMEM supplemented with 10% horse serum and 5% fetal calf serum at 37°C and 10% CO_2. Cells were transfected by electroporation as previously described (Kaether *et al*., 1997) using a Bio-Rad gene pulser (Bio-Rad, Hercules, CA). For microscopic analysis transfected PC12 cells were plated on poly-L-lysine (PLL, 0.1 mg/ml; Sigma Chemical)-coated LabTek chambered four-well coverglasses (Nalge Nunc; Wiesbaden, Germany) or 9-mm coverslips. For biochemical experiments transfected cells were plated on PLL-coated 100- or 140-mm dishes.

Fluorescence Labeling of Organelles

To fluorescently label SGs, PC12 cells were either transfected with pCDM8/hCgB-GFP(S65T) or with pcDNA3/hCgB-EGFP, plated on coated coverslips (immunofluorescence analysis) or on LabTek chambers (live cell imaging) and incubated in cell culture medium. Cells transfected with pCDM8/hCgB-GFP(S65T) were supplemented with 10 mM sodium butyrate for 17.5 h. The culture medium was replaced by block buffer (PBS supplemented with 1 mM $CaCl_2$ and 0.5 mM $MgCl_2$) and cells were incubated for 2 h at 20°C. To release the temperature block, the block buffer was replaced by culture medium prewarmed to 37°C and incubated for different chase times as indicated. Cells cotransfected with pcDNA3/hCgB-EGFP and pcDNA3/bFur were cultured for 2 h at 37°C and then incubated for 2 h at 20°C in block buffer and subsequently chased in prewarmed medium at 37°C as indicated in the presence of 10 μg/ml cycloheximide. To label peroxisomes with GFP, cells were transfected with pcDNA3/PTS1-GFP, plated on coated coverslips, and fixed 5 h after transfection. To fluorescently label mitochondria, untransfected cells were incubated for 1 h at 37°C in medium supplemented with 1 μM MitoTracker Red CM-H2Xros (#M-7513; Molecular Probes, Eugene, OR) and then fixed.

Depolymerization of Microtubules and F-Actin

To depolymerize microtubules, cells were incubated in block buffer supplemented with 10 μM nocodazole (stock solution: 2 mM nocodazole, 4% [vol/vol] dimethyl sulfoxide in PBS) for 1 h on ice and then for 2 h at 20°C. Subsequently the cells were chased by replacing the block buffer with culture medium prewarmed to 37°C and supplemented with 10 μM nocodazole. For long chase times the chase medium was replaced every 90 min. To depolymerize F-actin, cells were incubated for 2 h in block buffer at 20°C. During the last hour latrunculin-B was added to a final concentration of 5 μM (stock solution: 1 mM latrunculin-B, 10% [vol/vol] dimethyl sulfoxide in PBS). Subsequently, the cells were chased by replacing the block buffer with culture medium prewarmed to 37°C and supplemented with 5 μM latrunculin-B. For long chase times the chase medium was replaced every 90 min. For simultaneous depolymerization of microtubules and F-actin, cells were incubated for 2 h at 20°C in block buffer and then chased for 70 min in culture medium prewarmed to 37°C. Thereafter, the culture medium was replaced by medium containing 10 μM nocodazole and 5 μM latrunculin-B. After drug application (30 or 100 min) cells were fixed and stained for F-actin, Thy1.1, or TGN38.

Live Cell Imaging and Image Analysis

Transfected cells grown on PLL-coated LabTek chambers were imaged with the confocal Leica TCS 4D microscope equipped with an Ar/Kr laser, a 488/568 beamsplitter, and 525/50-nm bandpass emission filter and a 63×/1.40 NA PL APO objective lens. The fast scan mode at 512 × 512 pixel resolution was used. Video sequences of 20 frames were acquired at 0.56 frames/s. Movement of fluorescent SGs was manually quantified using the measure lengths algorithm of IPLab software, version 3.2.2 (Scanalytics, Fairfax, VA). The mean velocity of individual SGs was calculated from the observed trajectories. From all SGs per cell (at average 20) the mean velocities were averaged. For the velocity plots in Figure 4 at least five cells were evaluated per time window and condition. Two-dimensional

diffusion coefficients were calculated according to the equation $D = d^2/4t$, where D is the diffusion coefficient, d is the displacement of the object from the location of its first observation, and t is the observation period (Crank, 1975).

Quantitative Immunofluorescence Analysis

Indirect immunofluorescence labeling was performed as previously described (Wacker *et al.,* 1997). For Thy1.1 surface staining, detergent extraction with Triton X-100 was omitted. F-actin was fluorescently labeled with phalloidin-TRITC or phalloidin-FITC conjugate (250 nM final concentration). For microtubule-staining cells were preextracted before fixation by a 2-min incubation in preextraction buffer (0.5% [vol/vol] NP-40, 5 mM EGTA, 1 mM $MgCl_2$, 80 mM piperazine *N*,*N*′-bis(2-ethanesulfonic acid)/KOH pH 6.8). Cells were analyzed with a Leica TCS 4D confocal microscope equipped with an Ar/Kr laser, a 488/568 beamsplitter, 525/50-nm bandpass, and 590-nm longpass emission filters, and a 63×/1.4 NA PL APO objective lens. For quantitation of colocalizing signals 40 consecutive confocal slices at a resolution of 512 × 512 pixel were taken for each fluorochrome. The image data were transferred into IPLab software, version 3.2.2 and transformed into binary data sets as follows: in images containing GFP-, Mitotracker-, or immunofluorescence signals the background was set to zero and the positive signals to maximum value. Images containing Thy1.1 or F-actin staining were binarized by setting the threshold such that in confocal slices taken through the middle of the cell the positive signal formed a continuous, ring-like structure. This threshold was easily adjustable because both signals showed a steep intensity gradient from the cell periphery toward the cell center. Corresponding image pairs of the sequences were superimposed and rendered to a three-dimensional (3D) representation by IPLab3.2.2 3D-extension. Colocalization of SGs, peroxisomes, and mitochondria with the cortical area was quantitated from the 3D-representations.

RESULTS

ISGs Are Visualized by Means of a Pulse/Chase-like System

To monitor biogenesis of ISGs at the TGN and their subsequent transport to the PM we expressed hCgB-GFP(S65T) in PC12 cells. Previously, we had shown by radioactive pulse/chase labeling in combination with sucrose density gradient analysis that a similar GFP-fusion protein, hCgB-EGFP, was sorted with high specificity into ISGs (Kaether *et al.*, 1997). Using an identical protocol, we confirmed the same sorting specificity for hCgB-GFP(S65T) and furthermore, we found a characteristic increase in density of hCgB-GFP(S65T)-containing SGs after longer chase times, which is indicative of their maturation (our unpublished results).

After transfection of hCgB-GFP(S65T) in PC12 cells application of a 20°C secretion block for 2 h (referred to as pulse) led to a clustered perinuclear fluorescence signal (Figure 1A), which colocalized largely with the TGN marker protein TGN38 (Figure 1, B and C) (Luzio *et al.*, 1990). The few punctate fluorescence signals in this area most likely reflect aggregated hCgB-GFP(S65T) in the TGN because SG biogenesis is blocked at 20°C (our unpublished results; Xu and Shields, 1994). After reversal of the secretion block at 37°C (referred to as chase) the TGN38 staining remained as a clustered, perinuclear signal (Figure 1E). In contrast, the GFP-fluorescence showed in addition to the perinuclear signal numerous punctate structures throughout the cytoplasm (Figure 1D). Whereas the perinuclear GFP signal largely colocalized with the TGN38 staining the green puncta were devoid of TGN38, indicating biogenesis of fluorescent ISGs (Figure 1F). Importantly, fluorescent hCgB-GFP(S65T) generated during the secretion block at 20°C remained fluorescent under chase conditions at 37°C, whereas newly synthesized hCgB-GFP(S65T) was not converted to its fluorescent form at 37°C (our unpublished results). To analyze the time course of ISG biogenesis, cells were pulsed by a 20°C secretion block and fixed after different chase times up to 3 h. For each time point at least six cells were analyzed by confocal microscopy. Forty consecutive sections were taken per cell and rendered to three-dimensional representations (see MATERIALS AND METHODS). The total number of SGs per cell was counted and statistical analysis revealed a $t_{1/2}$ of 26 min for ISG biogenesis. The maximal number of fluorescent SGs per cell (147 ± 19 [mean ± SE; n = 6 cells]) was found after ~60 min of chase. At this time point the fluorescent hCgB-GFP(S65T) had completely exited from the TGN into ISGs. Thus, this system allows the generation of fluorescent SGs of a defined age.

Dynamics of ISGs Depends on Maturation Status

To study the transport of ISGs during the maturation period we performed confocal live cell microscopy. PC12 cells transfected with hCgB-GFP(S65T) were pulsed by a 20°C secretion block and imaged after different chase times up to 4 h. Confocal sections through the middle of the cells were found to be optimal for monitoring the traffic of ISGs from the TGN to the PM. The observed movements of the ISGs were manually tracked. Three characteristic features of transport were found. First, ISGs left the TGN on straight trajectories toward the PM with maximal velocities of up to 2 μm/s. This behavior was most frequently seen during the first 20 min of chase and is exemplified in Figure 2A (open arrowheads), which shows a track display of a cell imaged after 10 min of chase. Second, a random movement with reduced velocity (up to 0.7 μm/s) was detected in the cell periphery. This type of movement prevailed in a time window from 40 to 150 min of chase (Figure 2B, filled arrowheads) but was detectable through the entire observation period (Figure 2, A and C, filled arrowheads). Third, after ~160 min of chase the majority of SGs showed a very restricted movement as if they were tethered (Figure 2C, arrows). Restricted movements of ISGs were seen through the entire observation period (Figure 2B, arrows) although with significantly lower frequency.

Transport of Maturing SGs Is Microtubule- and Actin-dependent

The motility features of fluorescent SGs at different chase times prompted us to investigate the role of cytoskeletal elements in their trafficking. To address a role of microtubules, transport of fluorescent SGs was analyzed in the absence and presence of nocodazole. Two controls were included. First, it was confirmed by immunostaining of α-tubulin that most microtubules were depolymerized by nocodazole (our unpublished results). Second, the integrity of the TGN under these conditions was tested by antibody staining against the TGN marker protein TGN38. The obtained immunofluorescence signal was found to be perinuclear and clustered although slightly less compact as under control conditions (our unpublished results). Notably, in

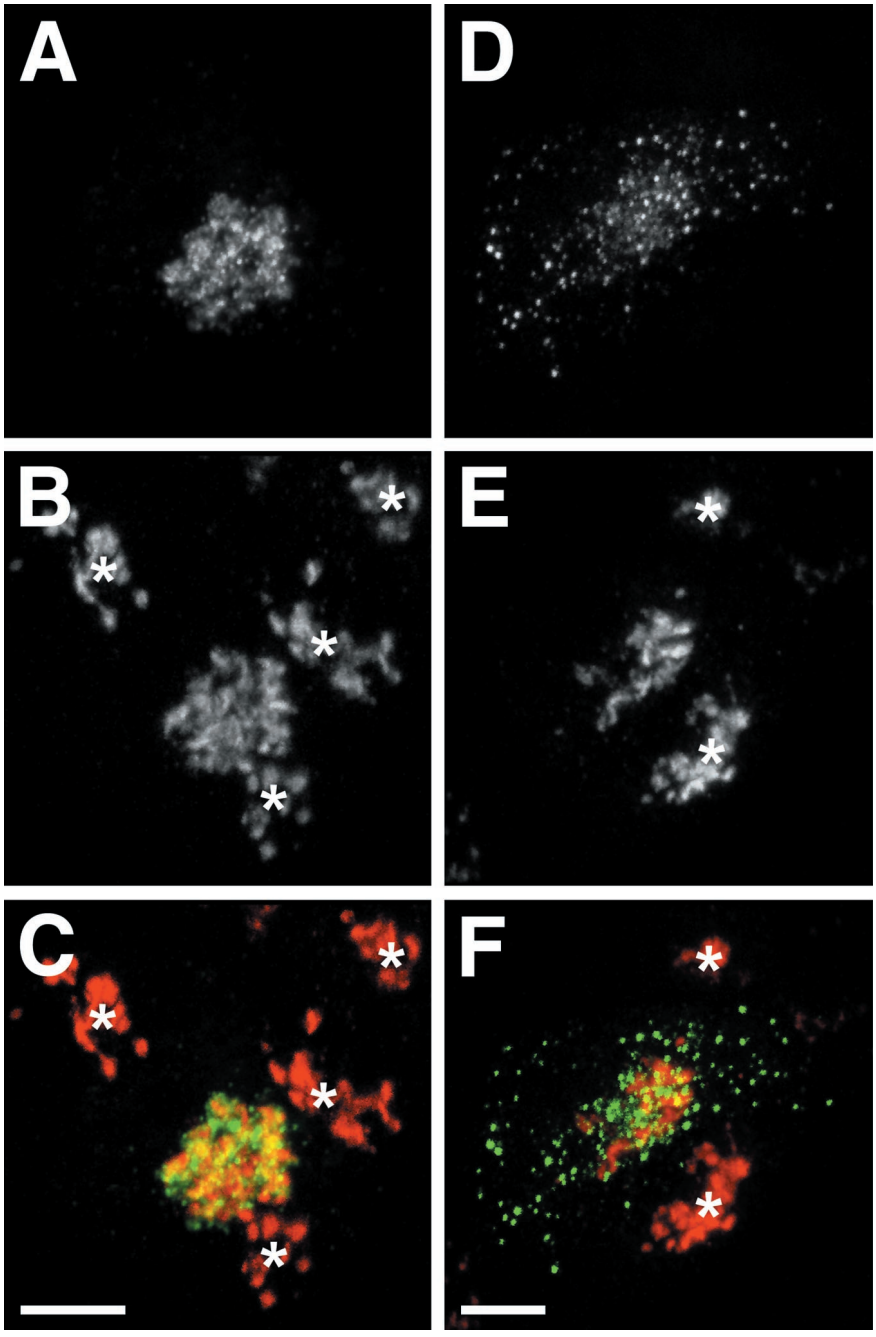

Figure 1. Generation and visualization of newly formed SGs. PC12 cells transfected with hCgB-GFP(S65T) were plated onto coverslips. Cells were incubated for 2 h at 20°C (temperature block) and either fixed (A–C) or incubated additionally for 30 min at 37°C (chase) and then fixed (D–F). After fixation, cells were immunostained for TGN38 protein and analyzed by confocal double fluorescence microscopy. Forty confocal sections per cell were taken and superimposed. (A and D) GFP-fluorescence. (B and E) TGN38 immunofluorescence. (C) Overlay of A (green) and B (red). (F) Overlay of D (green) and E (red). Yellow indicates colocalization of TGN38 and GFP-fluorescence. Asterisks mark TGN38 staining of cells that do not express hCgB-GFP. Bars, 5 μm.

hCgB-GFP(S65T) transfected cells chased for 30 min at 37°C in the presence of nocodazole, the TGN38 signal colocalized with the clustered, perinuclear GFP-fluorescence but not with green fluorescent punctate structures, which are indicative of fluorescent SGs (our unpublished results). Thus, in contrast to other cells such as NRK (Ho *et al.*, 1989) or BHK (Saraste and Svensson, 1991), the TGN of PC12 cells hardly disintegrates in the presence of nocodazole. This permitted an unequivocal identification of GFP-fluorescent punctate structures as ISGs.

To measure the influence of microtubules on SG transport, video sequences were taken at different chase times in the presence and absence of nocodazole and mean and maximal velocities of fluorescent SGs were determined. From the collected data the existence of discrete chase time windows with similar velocity values became evident. The values contained in these time windows were averaged and are depicted in Figure 3A. Several findings were made. In control cells a peak in mean velocity of 0.27 μm/s was found between 16 and 25 min of chase (Figure 3A, black bars). In

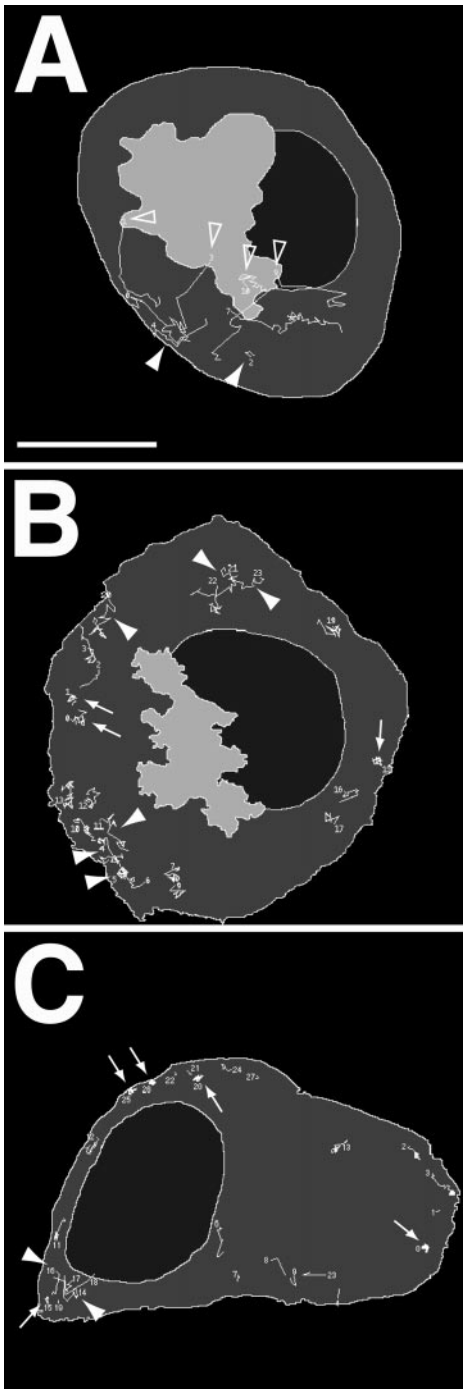

Figure 2. Three distinct features of SG movement are found during maturation. Cells transfected with hCgB-GFP(S65T) were incubated for 2 h at 20°C and then chased for various times at 37°C. Confocal live cell imaging was performed and SG movement was manually tracked. In the track displays the cell shape (dark gray), the nucleus (black) and the TGN (light gray) are outlined. Trajectories of newly born ISGs are indicated with open arrowheads (TGN-to-PM transport), SGs undergoing peripheral movement are indicated with filled arrowheads and immobilized SGs (coiled appearance) are exemplified by arrows. (A) A 10-min chase: newly formed SGs are transported straight from the TGN to the PM. (B) A 50-min chase: SGs frequently undergo short, random movement mostly in the vicinity of the PM. (C) A 180-min chase: most SGs show trajectories with coiled appearance mostly in the cell periphery. Bar, 5 μm. Video sequences illustrating the reported motility features are available at http://www.nbio.uni-heidelberg.de/Groups/WWW_Gerdes/publica.html.

contrast, this peak in mean velocity was absent in nocodazole-treated cells (Figure 3A, white bars). The corresponding histogram shows that >60% of SGs moved at low speed (<0.2 μm/s) and the number of SGs displaying fast movement (>0.3 μm/s) was significantly reduced (Figure 3B). At chase times between 40 to 150 min the effect of nocodazole on the mean velocity of SGs was less pronounced and was absent between 160 and 180 min of chase (Figure 3A). These data are consistent with the observation, that in the presence of nocodazole the transport of SGs from the TGN to the cell periphery was slow and resembled Brownian motion (our unpublished results). Taken together, our results suggest that microtubules are implicated particularly in the transport of ISGs from the TGN to the PM.

Next, the influence of F-actin on the dynamics of fluorescent SGs was tested. Transfected cells were imaged at different chase times in the presence or absence of latrunculin-B and for both conditions mean and maximal velocities of SGs were determined. Latrunculin-B efficiently depolymerized F-actin as tested by staining with TRITC-phalloidin (our unpublished results). The analysis of SG movement led to two main observations. First, during the initial 125 min of chase the mean velocities of SGs in cells treated with latrunculin-B were found to be very similar to those of control cells (Figure 3A). Second, in a time window between 126 and 180 min of chase, when the mean velocity decreased in control cells, a slight increase in mean velocity was observed in the presence of latrunculin-B (Figure 3A). In addition, fluorescent SGs in latrunculin-B treated cells but not in control cells showed directed movement with maximal velocities of up to 2 μm/s after 150 min of chase (our unpublished results). A quantitative analysis revealed that between 160 and 180 min of chase ~10% of SGs moved faster than 0.4 μm/s (Figure 3C). This suggests that at a late maturation status SGs are liberated from the peripheral area in the presence of latrunculin-B and thereby regain access to microtubule tracks. Taken together, our data suggest a consecutive action of microtubules and actin filaments: whereas microtubules particularly accomplish fast TGN to PM transport of newly formed ISGs, actin filaments play a role in transport or immobilization of SGs at later stages of maturation. However, we could show by gradient analysis that neither nocodazole nor latrunculin-B had an effect on the budding of ISGs from the TGN or the increase in density during maturation of ISGs (our unpublished results).

During Maturation Three Different Pools of SGs Are Formed

The observation that after 3 h of chase in latrunculin-B-treated cells the mean velocity of SGs was higher than in control cells (Figure 3A) prompted us to quantitate the amount of immobilized SGs as a function of chase time in the absence or presence of latrunculin-B. For this purpose

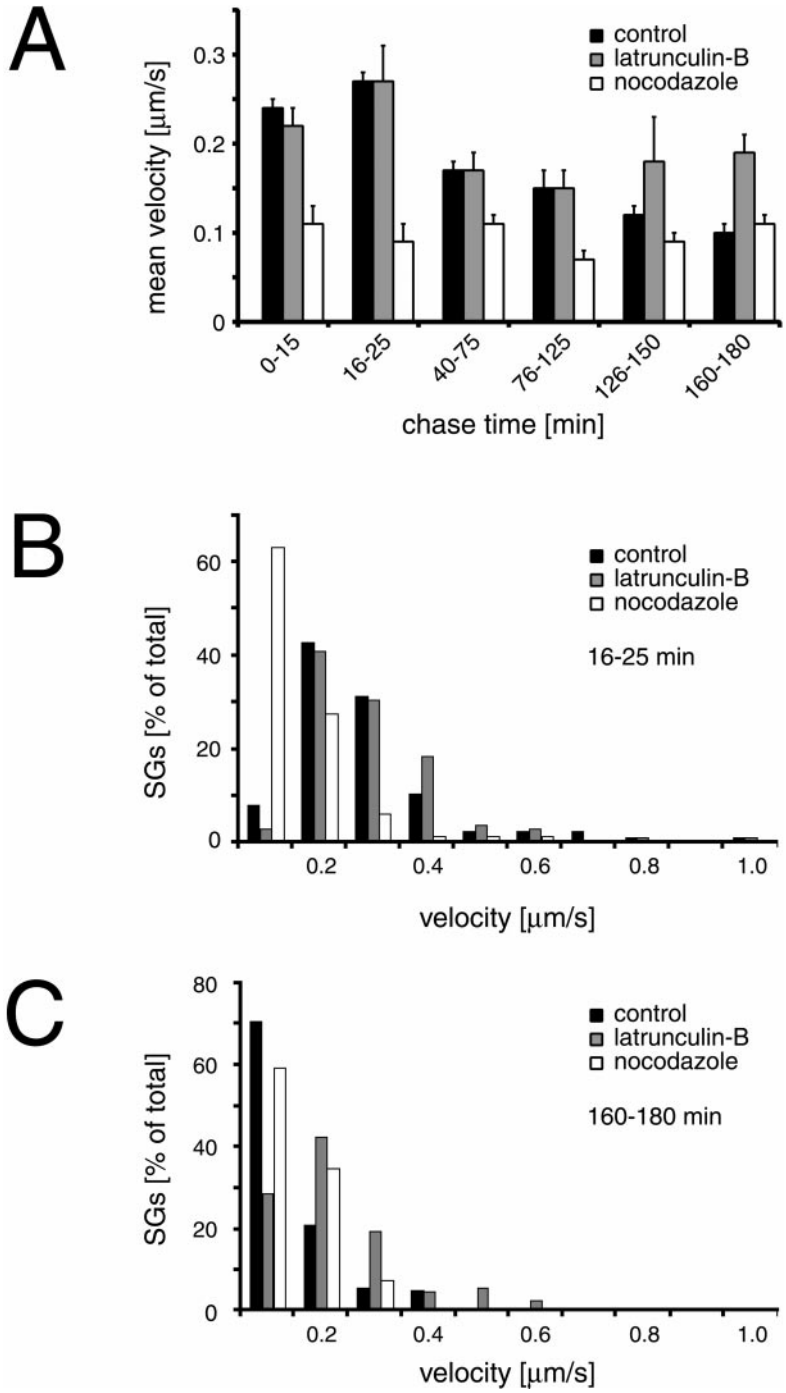

Figure 3. Transport of SGs is microtubule- and F-actin-dependent. Cells transfected with hCgB-GFP(S65T) were incubated for 2 h at 20°C and then chased at 37°C. Confocal live cell imaging was performed, movement of fluorescent SGs was manually tracked, and mean velocities were quantitated (see MATERIALS AND METHODS) from three independent experiments (A). The graph shows the mean velocities of SGs corresponding to the indicated time windows. Note, that in contrast to control cells 1) the velocity peak at early chase times is absent in the presence of nocodazole, and 2) the mean velocity after chase times >125 min increases in the presence of latrunculin-B. Two histograms corresponding to the 16–25-min and 160–180-min chase time windows show the percentage of SGs as a function of velocity in B and C, respectively (number of SGs >80 for each condition). Error bar, SE.

the diffusion coefficients (D) of fluorescent SGs were calculated under the respective conditions. SGs were classified according to their D-values. A pool of SGs with $D \geqq 1 \times 10^{-10}$ cm^2/s was found during the entire observation period of 3 h and was termed mobile. SGs with $D < 1 \times 10^{-10}$ cm^2/s showed, in contrast to the mobile pool, trajectories with a characteristic coiled appearance and were therefore termed immobile (Figure 2C, arrows). Quantitation as a function of chase time revealed under control conditions an increase of immobile SGs in two steps. One increase from a low level of 8 ± 2% (mean ± SE; n = 8 cells) to 29 ± 5% (mean ± SE; n = 10 cells) of total became evident between 40 and 75 min of chase (Figure 4A). We refer to this as pool IP1. A second increase to a plateau value of 67 ± 5% (mean ± SE; n = 10 cells) was detected between 160 and 180 min of chase (Figure 4A). This pool was termed IP2. Interestingly, latrun-

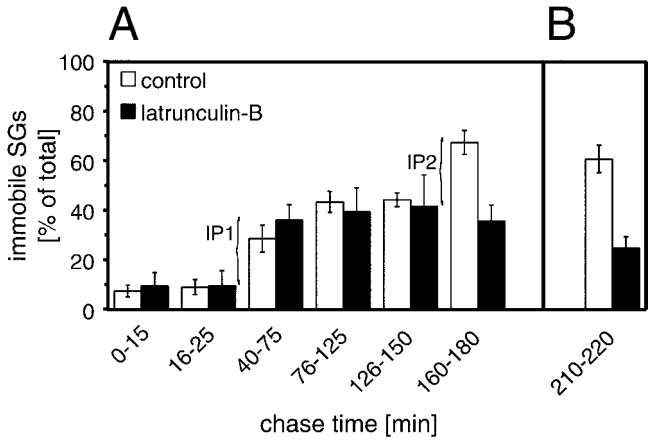

Figure 4. Immobilization of SGs after long chase times is F-actin-dependent. Cells transfected with hCgB-GFP(S65T) were incubated for 2 h at 20°C and then chased at 37°C in the absence or presence of latrunculin-B as indicated. Latrunculin-B was added at the beginning of the temperature block (A) or after 3 h of chase (B). Confocal live cell imaging was performed, movements of fluorescent SGs were manually tracked, and diffusion coefficients were calculated (see MATERIALS AND METHODS). The percentage of fluorescent SGs exhibiting a value of $< 10^{-10}$ cm^2/s (referred to as immobile) was determined for the indicated chase time windows. Data of three independent experiments are shown. Error bar, SE. Note, that 1) in control cells the percentage of immobile fluorescent SGs significantly increased between 40 and 75 min (referred to as IP1 pool) and 160 and 180 min of chase (IP2 pool), and 2) the IP2 pool is absent in the presence of latrunculin-B. The pools are indicated by curved brackets.

culin-B did not affect the formation of IP1 but prevented formation of IP2 (Figure 4A). To test whether latrunculin-B not only prevents but also reverses immobilization of SGs at late time points, cells were first chased for 3 h under control conditions and then for 30–40 min in the presence of latrunculin-B and subsequently imaged. As shown in Figure 4B, the immobile pool of SGs was reduced from the control value of 61 ± 5% (mean ± SE; n = 6 cells) to 25 ± 5% (mean ± SE; n = 6 cells) of total. Thus, latrunculin-B completely reversed the F-actin-dependent immobilization at late chase times. This strongly suggests that SGs undergo both F-actin independent and F-actin dependent immobilization. Furthermore, the narrow time window for F-actin-dependent immobilization indicates that this process is tightly linked to the maturation status of SGs.

ISGs Are Restricted to the Cell Cortex

In PC12 cells the majority of MSGs is localized in proximity to the plasma membrane (Banerjee *et al.*, 1996), the site of docking and exocytosis (Martin and Kowalchyk, 1997). However, it is unknown whether ISGs are also located in this area. Therefore, we studied the subcellular distribution of SGs during maturation in more detail. In particular we determined the degree of colocalization of SGs with cortical F-actin as a function of maturation time. After application of the 20°C temperature block, hCgB-GFP(S65T) transfected cells were chased for different time periods, fixed, and stained with phalloidin-TRITC for F-actin. Figure 5A shows a confocal section of a cell after 10 min of chase where the fluorescent TGN appears as a green cluster and newly formed SGs as punctate structures. Already at this early time point most SGs colocalized with the ribbon-like actin cortex (Figure 5A, arrowheads) and only a few were not located in the cortical region (Figure 5A, arrows). To determine the extent of colocalization as a function of chase time, at least six cells were analyzed for each time point. To gain a reliable evaluation, colocalization was quantitated from three-dimensional representations of cells obtained from 40 consecutive confocal sections per cell (see MATERIALS AND METHODS). Notably, already after 2 min of chase ~70% of SGs were found to colocalize with the cortical F-actin (Figure 5G). The extent of colocalization reached a plateau of ~80% after 100 min of chase and thereafter remained constant over the analyzed time period of 3 h (Figure 5, B and G). The distribution of peroxisomes labeled with GFP fused to the peroxisomal targeting signal 1 (Figure 5D) or mitochondria labeled with Mitotracker (Figure 5E) was different compared with newly formed SGs. Peroxisomes colocalized to 41% (Figure 5G, dotted line) and mitochondria to 23% (Figure 5G, dashed line) with F-actin. This indicates that the high concentration of fluorescent SGs in the cortex was not due to limited space in the relatively small PC12 cell.

Because we had found a microtubule-dependent, unidirectional transport to the cell periphery (Figure 2A), it was conceivable that this centrifugal movement was the underlying cause for the cortical localization of fluorescent SGs. To test this possibility, we analyzed whether the absence of microtubules would lead to a lower degree of cortical localization. Therefore, colocalization of fluorescent SGs with cortical F-actin was quantitated in nocodazole-treated PC12 cells after 2, 10, 100, and 170 min of chase. Although for all measured time points the extent of colocalization seemed to be slightly reduced compared with control conditions (Figure 5G; *t* test, $p < 0.05$) between 60 and 70% of fluorescent SGs were detected in the F-actin-rich cortex. We then investigated whether the tight network of cortical F-actin itself was involved in the restriction of SGs to the cell periphery. We made use of latrunculin-B to efficiently depolymerize F-actin and immunostained the PM with an antibody against Thy-1.1 to evaluate the cortical localization of fluorescent SGs in the absence of F-actin. The validity of this PM marker was confirmed under control conditions where a double immunofluorescence analysis resulted in a strong overlap of immunostained Thy-1.1 and phalloidin-stained F-actin (Figure 5F). Furthermore, in control cells the amount of colocalization of fluorescent SGs with either F-actin or Thy-1.1 was very similar (Figure 5G, compare black and gray bars). Interestingly, incubation of cells with latrunculin-B led only to a slight decrease in cortical localization of fluorescent SGs (Figure 5G; *t* test, $p < 0.05$). This effect was very similar to that of nocodazole. However, when cells were simultaneously treated with latrunculin-B and nocodazole, a substantial decrease of fluorescent SGs in the cortex was observed, which was paralleled by an increase of fluorescent SGs in the interior of the cell (Figure 5C). It was confirmed that under these conditions the cells were still viable because repolymerization of microtubules and F-actin was observed when cells were incubated for an additional hour in the absence of both drugs (our unpublished results). Quantitative analysis of cells in the presence of nocodazole

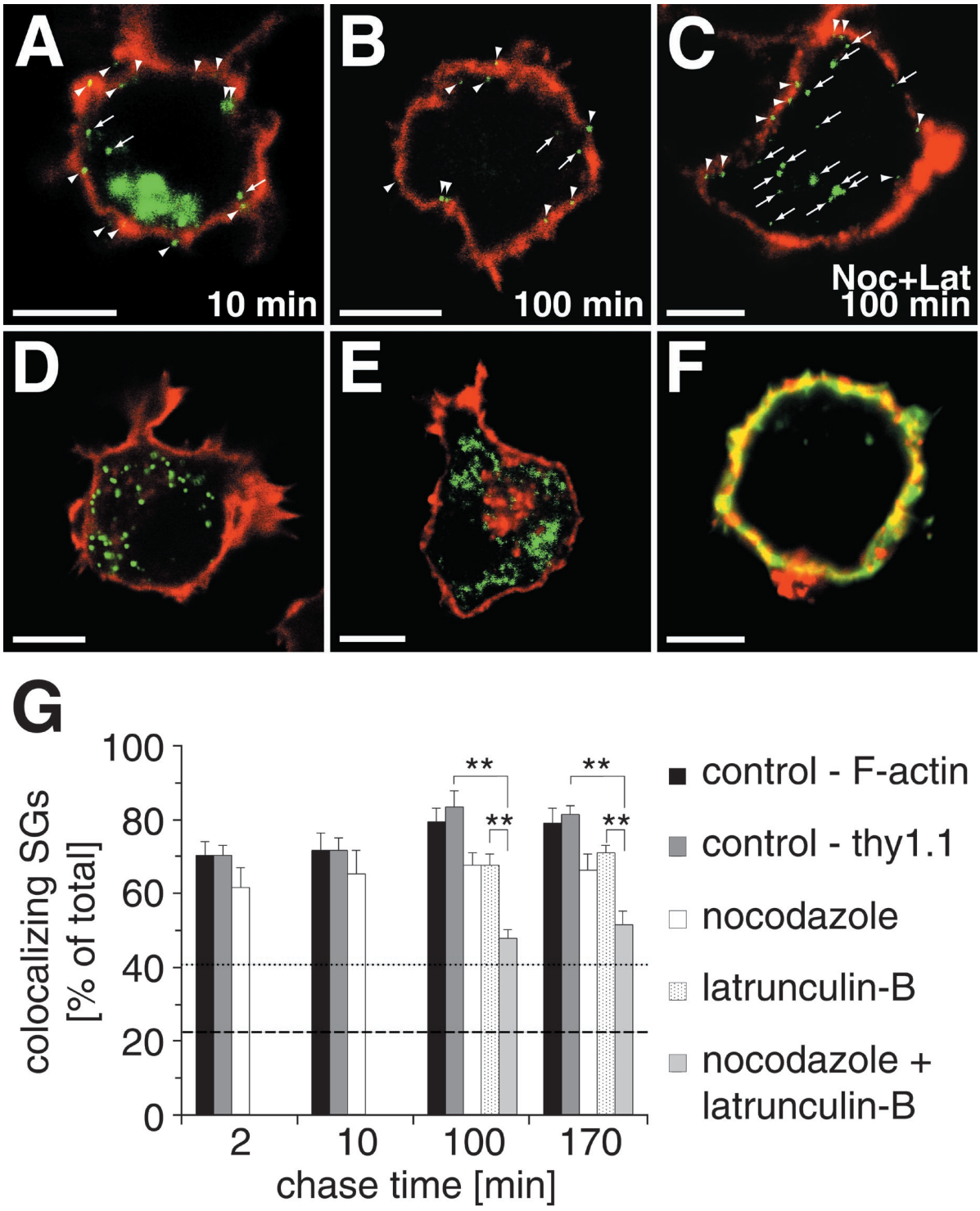

Figure 5. SGs are restricted to the F-actin-rich cell cortex during maturation. The colocalization of hCgB-GFP(S65T)-fluorescent SGs (A–C), peroxisomes (D), or mitochondria (E) with F-actin (A, B, D, and E, red signal) or immunostained Thy1.1 (C, red signal) was analyzed. Arrowheads and arrows indicate colocalizing and noncolocalizing organelles, respectively, with cortical staining. (F) A cell double-stained with FITC-phalloidin (green) and anti-Thy1.1 (red). Note the extensive colocalization (yellow) of both markers. (A–C) Cells transfected with hCgB-GFP(S65T) were incubated for 2 h at 20°C, chased for indicated times in the absence (A and B) or presence (C) of nocodazole and latrunculin-B (for details see MATERIALS AND METHODS), fixed, and then stained for the cortex (F-actin or Thy1.1). The clustered green fluorescence in A indicates the TGN, the green puncta in A–C represent fluorescent SGs. (D) Cells transfected with PTS1-GFP show green

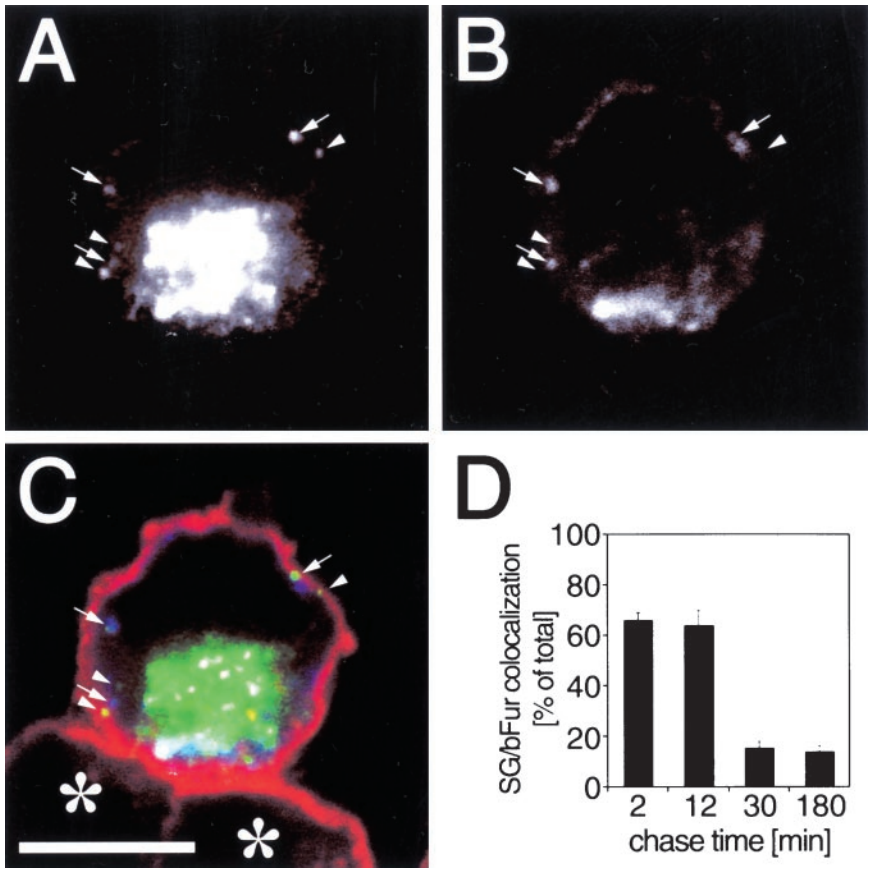

Figure 6. Furin-containing SGs colocalize with the F-actin-rich cortex. Two hours after cotransfection of hCgB-EGFP and bFur PC12 cells were incubated for 2 h at 20°C and chased for different time periods at 37°C. Then cells were processed for fluorescence labeling and analyzed by confocal microscopy. (A–C) A single confocal section of a cell chased for 12 min and triple-labeled with hCgB-EGFP, immunostained bfur, and TRITC-phalloidin–stained F-actin. (A and B) Single channel recordings of hCgB-EGFP and immunostained bFur, respectively. (C) Overlay of hCgB-EGFP (green), bfur (blue), and TRITC-phalloidin–labeled F-actin (red). Arrows, punctate hCgB-EGFP signals colocalizing with bFur signals; arrowheads, punctate hCgB-EGFP signals not colocalizing with bFur; asterisks, nontransfected cells; bar, 5 μm. Note that the clustered, perinuclear fluorescence signal in A–C indicates the TGN. (D) For a quantitative analysis of colocalization cells were chased for indicated time periods, fixed, and immunostained for bFur. Colocalization of green fluorescent SGs with punctate bFur signals was analyzed by the use of 3D software (see MATERIALS AND METHODS). For each time point at least six cells from two independent experiments (≧ 190 SGs per time point) were quantified. Error bars, SE.

and latrunculin-B revealed that after 100 and 170 min 48 ± 2% (mean ± SE; n = 6 cells) and 51 ± 4% (mean ± SE; n = 6 cells) of SGs remained in the cell cortex, respectively (Figure 5G). These values were significantly lower (*t* test, $p < 0.01$) than those obtained for control cells or for cells treated with either nocodazole or latrunculin-B alone. On the other hand, the combined action of latrunculin-B and nocodazole resulted in a higher value of cortical localization of fluorescent SGs as was observed for mitochondria in untreated cells (23%, dashed line in Figure 5G). Thus, our data suggest that both microtubules and F-actin synergistically affect the cortical localization of SGs during their maturation.

Figure 5 (cont). fluorescent peroxisomes. (E) Cells incubated with Mitotracker show fluorescent mitochondria (shown in green). The red staining in the TGN area visible in some but not all cells indicates the presence of F-actin. (G) Quantitative analysis of colocalization. For each condition, cells were analyzed by confocal sectioning. The amount of colocalization between cortical markers and hCgB-GFP(S65T)-fluorescent SGs (bars), peroxisomes (dotted line) or mitochondria (dashed line) was determined by the use of 3D software (see MATERIALS AND METHODS). Error bars, SE. Significance ($p < 0.01$) is indicated by **. For all conditions at least six cells from two independent experiments were quantified. Note that in the presence of latruculin-B or latrunculin-B plus nocodazole cells were only analyzed after 100 and 170 min of chase.

ISGs Complete Maturation in the F-Actin–rich Cell Cortex

To directly address whether newly formed granules are still immature when reaching the cell cortex, we looked for their colocalization with furin, an endoprotease known to be present in ISGs but not in MSGs (Dittie *et al.*, 1997). Because endogeneous furin is hardly detectable, we expressed bFur together with hCgB-EGFP and analyzed the cells by triple color fluorescence microscopy as illustrated in Figure 6, A–C. Strikingly, after 12 min of chase, newly formed SGs frequently colocalized with bFur (Figure 6, A and B, arrows) and with cortical F-actin (Figure 6C). This indicates that SGs did not complete maturation before arrival at the cell cortex. Interestingly, no difference in cortical localization was found between bFur-positive (Figure 6C, arrows) and bFur-negative fluorescent SGs (Figure 6C, arrowheads). Because it is known from biochemical experiments that furin is removed from SGs during the course of their maturation (Dittie *et al.*, 1997), we quantified the colocalization of hCgB-EGFP-labeled SGs with punctate signals of bFur as a function of chase time. A high colocalization of 66 ± 3% (mean ± SE; n = 6 cells) and 64 ± 6% (mean ± SE; n = 6 cells) was obtained after 2 and 12 min of chase, respectively (Figure 6D). Already after 30 min of chase the colocalization of bFur and fluorescent SGs was significantly lower (16 ± 3% [mean ± SE; n = 6 cells]) and stayed constant up to at least 180 min of chase (Figure 6D). A similarly low value of 14 ±

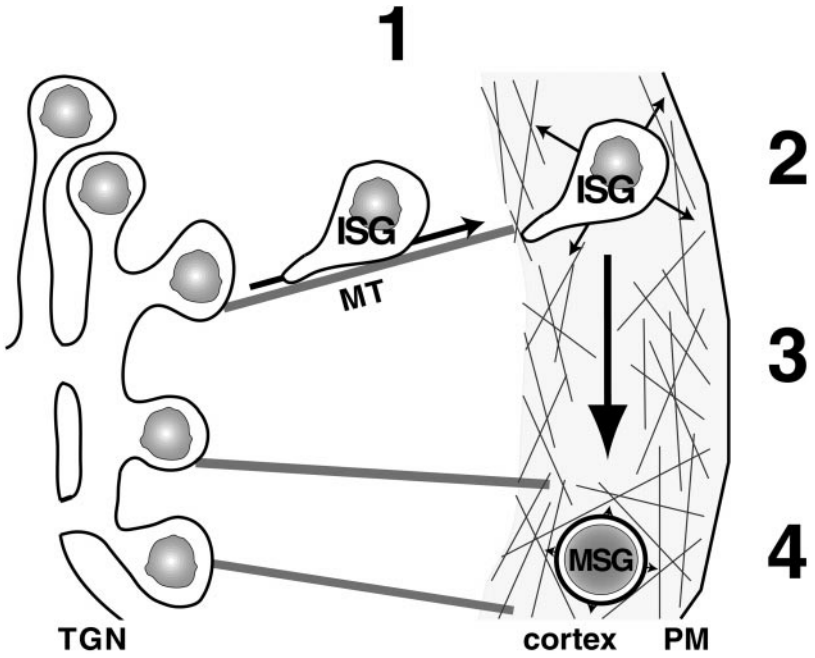

Figure 7. Model of SG transport and distribution during maturation. (1) Newly formed ISGs are transported in a microtubule-dependent and one end-directed manner from the TGN toward the cell periphery. (2) SGs are captured in the F-actin-rich cell cortex where they move randomly (indicated by arrows). (3) SGs mature within the F-actin-rich cortex (big arrow). (4) At the end of maturation a significant proportion of SGs undergoes F-actin-dependent immobilization, resulting in oscillation around a center of gravity (indicated by arrowheads). MT, microtubule.

3% (mean ± SE; n = 6 cells) colocalization between fluorescent SGs and Alexafluor 594-transferrin, a marker for endosomes that is not present in SGs, was found (our unpublished results). Because furin is known to retrieve from the PM to the TGN via the endosomal pathway, the residual value of colocalization between fluorescent SGs and bFur beyond 30 min of chase most likely reflects random colocalization due to the abundance of endosomal labeling. Taken together, these data strongly suggest that the majority of ISGs mature in the F-actin-rich cortex. Furthermore, the fluorescence analysis indicates that the maturation step resulting in the removal of furin occurs between 12 and 30 min of chase.

DISCUSSION

Visualization of ISGs

In the past, ISGs were studied biochemically by radioactive pulse/chase labeling in combination with subcellular fractionation (Tooze *et al.*, 1991). It has been shown by analytical differential centrifugation that after 15 min of chase ISGs exhibited a sedimentation behavior characteristic of a single, homogeneous population of particles (Tooze *et al.*, 1991; Bauerfeind *et al.*, 1993). Furthermore, it has been demonstrated biochemically that furin is present on ISGs but not on MSGs (Dittie *et al.*, 1997), and that its removal from ISGs is indicative of their maturation (Dittie *et al.*, 1997). The pulse/chase-like system described here facilitates the visualization of ISGs. The immature state of the majority of newly formed SGs was directly shown at the single granule level by colocalization with furin. Furthermore, the finding that fluorescent SGs colocalized to a much larger extent with furin at early compared with late chase times provides, in addition to the observed density shift on gradients (our unpublished results), a second criterion that fluorescent ISGs undergo maturation. Therefore, the pulse/chase-like system permits the visualization of newly formed ISGs in living cells and facilitates the generation of ISGs of a defined maturation status. The application of this system led to insights as to where ISG maturation occurs and permitted a detailed study of ISG dynamics.

Microtubule-dependent Transport of ISGs

It is generally accepted that transport of SGs over long distances as it occurs in neurites is facilitated by microtubules. This has been directly demonstrated in neurites of AtT20 cells for acridine orange-stained SGs (Kreis *et al.*, 1989). Whether microtubule-dependent transport plays also a role in small undifferentiated PC12 cells and moreover whether newly born ISGs are already equipped with the machinery necessary for microtubule-dependent transport is not clear. The finding that stimulated exocytosis of ISGs is delayed when PC12 cells are treated with nocodazole supports the view that microtubules are implicated in ISG transport (Tooze *et al.*, 1991). Our system enabled us to directly visualize the transport of ISGs from the TGN to the PM. A peak of velocity at early chase times in combination with a fast, directed transport of newly formed ISGs to the PM within 3 to 5 s, both absent in the presence of nocodazole, strongly suggest that TGN-to-PM transport is facilitated by microtubules (Figure 7). Theoretical considerations suggest that the distance of a few micrometers from TGN to PM in undifferentiated PC12 cells can be traversed by ISGs within minutes by Brownian movement (Bloom and Goldstein, 1998). Our observation that in the presence of nocodazole ISGs do not accumulate in the TGN area but reach the PM on zig-zag tracks (our unpublished results) is consistent with this view although actin-dependent transport cannot be excluded. Thus, although microtubule tracks do not seem to be

required for TGN-to-PM transport they are used by ISGs in undifferentiated PC12 cells.

The straight, unidirectional transport of newly formed ISGs toward the PM (Figure 7) contrasts with TGN-to-PM transport of constitutive vesicles, which is also microtubule-dependent but occurs in a random bidirectional manner (Wacker *et al.*, 1997). This may suggest that both kinesin and dynein are implicated in the transport of constitutive vesicles, whereas kinesin-dependent transport may prevail for ISGs. Interestingly, in neurites of NGF-differentiated PC12 cells, SGs were observed to move both anterogradely and retrogradely (Lochner *et al.*, 1998; Rudolf and Gerdes, unpublished results). The latter finding is consistent with the observed bidirectional movement of SGs in neurites of AtT20 cells (Kreis *et al.*, 1989).

Cortical Localization of ISGs

A remarkable finding of our study is that most SGs were found in the F-actin-rich cortex during the first 3 h after biogenesis. The characteristic increase in density of SGs as well as the removal of furin from SGs during this time span (Figure 6D) strongly suggests that ISG maturation takes place in the F-actin-rich cortex. Furthermore, our data suggest that the cortical restriction of ISGs is achieved by microtubules and F-actin. Whereas microtubules provide a fast and efficient transport system into the actin cortex, the latter facilitates efficient capturing of ISGs in the tight cortical F-actin network (Figure 7). Our results show that either of these mechanisms alone suffices to restrict most of the ISGs to the cell periphery. Peripheral localization during the absence of F-actin may be explained by a permanent and efficient microtubule-dependent force that propels ISGs continuously toward the cell periphery (Figure 7). Peripheral localization during the absence of microtubules may be envisaged by a slow and random transport of SGs by Brownian motion combined with efficient capturing in the cortex by an F-actin-dependent mechanism.

Our results corroborate a model of cooperative microtubule- and F-actin-dependent transport (Kuznetsov *et al.*, 1992; Rodionov *et al.*, 1998; Rogers and Gelfand, 1998; Wu *et al.*, 1998; reviewed by Brown, 1999). According to this model, microtubules facilitate a long-range transport, whereas actin filaments accomplish short-range transport in the cell periphery (reviewed by Brown, 1999) (Figure 7). This cooperativity leads to an efficient aggregation–dispersion mechanism for pigment-containing granules in melanophores of fish (Rodionov *et al.*, 1998) or *Xenopus* (Rogers and Gelfand, 1998). Recently, Hammer and colleagues have extended this model by proposing a capture function for actin-dependent transport of melanosomes (Wu *et al.*, 1998), leading to a polarized, uneven distribution of melanosomes in the dendritic arbor of mouse melanocytes. In essence, the cooperativity of microtubules and actin filaments seems to be a basic theme, which is adapted to the special needs of a cell-like dispersion and aggregation of melanosomes. Along these lines the localization of SGs in PC12 cells provides a good example of how this cooperativity leads to an extensive cortical distribution. In contrast to the described systems in melanocytes of fish and mouse where antagonistic action of the two transport systems have been observed, our data support the view that outward microtubule-dependent transport together with F-actin-dependent capturing synergistically mediate the cortical localization of SGs.

Previously, the cortical area was perceived as the site of priming and docking of MSGs (Robinson and Martin, 1998). We show that also ISGs are localized to this area. Although the relevance of this cortical localization of ISGs is unclear, our data imply that the complex process of ISG maturation occurs mainly in the F-actin-rich cortex. This was directly shown for one maturation step, namely, the removal of furin from ISGs, which was observed between 12 and 30 min of chase. Most likely also other proposed maturation steps such as homotypic fusion of ISGs and budding of ISG-derived vesicles from ISGs take place in the cortical region. The fusion of ISGs is postulated to be an important prerequisite for post-TGN sorting of proteins from maturing ISGs (Urbé *et al.*, 1998). In this context, the observed peripheral localization of ISGs in combination with a random movement may be advantageous for homotypic fusion because it provides a higher local concentration of this short-lived vesicular intermediate. Although direct evidence for ISG–ISG fusion was only obtained in vitro (Urbé *et al.*, 1998), live cell imaging of these immature organelles in PC12 cells showed rare events consistent with ISG–ISG fusion in the cortical area (Rudolf and Gerdes, unpublished results).

Pools of SGs

With our pulse/chase-like system we observed that the motility of ISGs changed as a function of chase time, which correlates with preceding maturation. Three distinct pools of SGs were characterized according to their motility or their mode of immobilization. One mobile pool with a $D \geqq 5 \times 10^{-10}$ cm^2/s is present during the entire maturation period (Figure 4, A and B) and two immobile pools, IP1 and IP2, share the same diffusion coefficient of $D < 10^{-10}$ cm^2/s but differ in the nature of their immobilization. The formation of the IP1 pool between 40 and 75 min of chase may depend on the specific maturation status of ISGs during this time. However, it is also possible that the detection of IP1 reflects a change in ratio between immobile and mobile ISGs, which is due to completion of exit of fluorescent hCgB-GFP(S65T) from the TGN at this time point.

Whereas our data do not give any insights about the formation of IP1 we obtained evidence that both the recruitment and maintenance of IP2 is F-actin-dependent (Figure 4, A and B). Interestingly, IP2, which contains ~25% of fluorescent SGs, was formed within a short time window. This suggests that the recruitment to IP2 requires a certain maturation status of ISGs, leading to a direct or indirect binding to F-actin. In the absence of F-actin, we observed at this time point not only liberation of immobile SGs but also fast directed tracks. Most likely, upon arrival, ISGs are captured in the F-actin-rich cortex, which prevents ISG-microtubule interaction. Similar observations were made for murine melanosomes (Wu *et al.*, 1998).

In neuroendocrine chromaffin (Trifaró and Vitale, 1993) and PC12 cells interaction of SGs with cortical F-actin has been reported (Trifaró and Vitale, 1993) and was found to be preserved in PM sheets of PC12 cells rich in F-actin (Martin and Kowalchyk, 1997; Avery *et al.*, 2000). In these studies however, SGs were analyzed under steady-state conditions, i.e., the obtained data were mostly based on the analysis of MSGs. With respect to the identified IP2 in our study it will

be of interest to biochemically characterize molecular components leading to the F-actin-dependent immobilization.

Furthermore, it will be of interest to investigate possible physiological roles of the SG pools observed here. It may be conceivable that these pools are implicated in the regulation of the turnover or exocytosis of SGs. Because biochemical studies have shown that ISGs are competent for exocytosis already 30 min after biogenesis (Tooze *et al.*, 1991), it may be speculated that the pools observed here respond differentially to stimulation. In this respect, electrophysiological studies in chromaffin cells (Neher and Zucker, 1993; Parsons *et al.*, 1995) and melanotrophs (Parsons *et al.*, 1995) revealed the existence of different SG pools, which differ in their response time to stimulation. In particular a readily releasable pool leading to an exocytotic burst within milliseconds and slower reacting pool(s) facilitating long-lasting exocytosis under sustained stimulation are described. Future studies will show whether the SG pools described here reflect morphological correlates of the pools identified by electrophysiological means.

ACKNOWLEDGMENTS

We thank D. Corbeil, D. Langosch, and E. Tanaka for critical comments on the manuscript; G. Banting for TGN38 antibody; W. Just for the PTS1-GFP cDNA; and W. Garten for bFur cDNA and bFur antibodies. We are also grateful to W.B. Huttner for continuous support. R.R. was supported by the "Studienstiftung des Deutschen Volkes" and T.S. by a "Stipendium by the Landesgraduiertenförderungsgesetz". H.-H.G. was a recipient of a grant from the Deutsche Forschungsgemeinschaft (SFB 317/C7 and SFB 488/B2).

REFERENCES

Avery, J., Ellis, D., Lang, T., Holroyd, P., Riedel, D., Henderson, R., Edwardson, M., and Jahn, R. (2000). A cell-free system for regulated exocytosis in PC12 cells. J. Cell Biol. *148*, 317–324.

Banerjee, A., Barry, V.A., Bibhuti, R.D., and Martin, T.F.J. (1996). N-ethylmaleimide-sensitive factor acts at a prefusion ATP-dependent step in Ca^{2+}-activated exocytosis. J. Biol. Chem. *271*, 20223–20226.

Bauerfeind, R., Régnier-Vigouroux, A., Flatmark, T., and Huttner, W.B. (1993). Selective storage of acetylcholine, but not catecholamines, in neuroendocrine synaptic-like microvesicles of early endosomal origin. Neuron *11*, 105–121.

Bloom, G.S., and Goldstein, L.S.B. (1998). Cruising along microtubule highways: how membranes move through the secretory pathway. J. Cell Biol. *140*, 1277–1280.

Brown, S. (1999). Cooperation between microtubule- and actin-based motor proteins. Annu. Rev. Cell Dev. Biol. *15*, 63–80.

Crank, J. (1975). The Mathematics of Diffusion, New York: Oxford University Press.

Dittie, A.S., Hajibagheri, N., and Tooze, S.A. (1996). The AP-1 adaptor complex binds to immature secretory granules from PC12 cells, and is regulated by ADP-ribosylation factor. J. Cell Biol. *132*, 523–536.

Dittie, A.S., Thomas, L., Thomas, G., and Tooze, S.A. (1997). Furin is sorted into the regulated secretory pathway in neuroendocrine cells, interacts with the AP-1 complex, and is removed during granule maturation by a casein kinase II dependent mechanism. EMBO J. *16*, 4859–4870.

Han, W., Ng, Y.-K., Axelrod, D., and Levitan, E.S. (1999). Neuropeptide release by efficient recruitment of diffusing cytoplasmic secretory vesicles. Proc. Natl. Acad. Sci. USA *96*, 14577–14582.

Heumann, R., Kachel, V., and Thoenen, H. (1983). Relationship between NGF-mediated volume increase and "priming effect" in fast and slow reacting clones of PC12 pheochromocytoma cells. Exp. Cell Res. *145*, 179–190.

Ho, W., Allan, V., van Meer, G., Berger, E., and Kreis, T. (1989). Reclustering of scattered Golgi elements occurs along microtubules. Eur. J. Biol. *48*, 250–263.

Huber, C., Saffrich, R., Anton, M., Paβreiter, M., Ansorge, W., Gorgas, K., and Just, W. (1997). A heterotrimeric G protein-phospholipase A_2 signaling cascade is involved in the regulation of peroxisomal motility in CHO cells. J. Cell Sci. *110*, 2955–2968.

Kaether, C., and Gerdes, H.-H. (1995). Visualization of protein transport along the secretory pathway using green fluorescent protein. FEBS Lett. *369*, 267–271.

Kaether, C., Salm, T., Glombik, M., Almers, W., and Gerdes, H.-H. (1997). Targeting of green fluorescent protein to neuroendocrine secretory granules: a new tool for real time studies of regulated protein secretion. Eur. J. Cell Biol. *74*, 133–142.

Klumperman, J., Kuliawat, R., Griffith, J.M., Geuze, H.J., and Arvan, P. (1998). Mannose 6-phosphate receptors are sorted from immature secretory granules via adaptor protein AP-1, clathrin, and syntaxin 6-positive vesicles. J. Cell Biol. *141*, 359–371.

Kreis, E.K., Matteoni, R., Hollinshead, M., and Tooze, J. (1989). Secretory granules and endosomes show saltatory movement biased to the anterograde and retrograde directions, respectively, along microtubules in AtT20 cells. Eur. J. Cell Biol. *49*, 128–139.

Kuznetsov, S.A., Langford, G.M., and Weiss, D.G. (1992). Actin-dependent organelle movement in squid axoplasm. Nature *356*, 722–725.

Lang, T., Wacker, I., Steyer, J., Kaether, C., Wunderlich, I., Soldati, T., Gerdes, H.-H., and Almers, W. (1997). Ca^{2+}-triggered peptide secretion in single cells imaged with green fluorescent protein and evanescent-wave microscopy. Neuron *18*, 857–863.

Lang, T., Wacker, I., Wunderlich, I., Rohrbach, A., Giese, G., Soldati, T., and Almers, W. (2000). Role of actin cortex in the subplasmalemmal transport of secretory granules in PC-12 cells. Biophys. J. *78*, 2863–2877.

Lochner, J.E., Kingma, M., Kuhn, S., Meliza, C.D., Cutler, B., and Scalettar, B.A. (1998). Real-time imaging of the axonal transport of granules containing a tissue plasminogen activator/green fluorescent protein hybrid. Mol. Biol. Cell *9*, 2463–2476.

Luzio, J.P., Brake, B., Banting, G., Howell, K.E., Braghetta, P., and Stanley, K.K. (1990). Identification, sequencing and expression of an integral membrane protein of the trans-Golgi network (TGN38). Biochem. J. *270*, 97–102.

Martin, T.F.J., and Kowalchyk, J.A. (1997). Docked secretory vesicles undergo Ca2+-activated exocytosis in a cell-free system. J. Biol. Chem. *272*, 14447–14453.

Neher, E., and Zucker, R.S. (1993). Multiple calcium-dependent processes related to secretion in bovine chromaffin cells. Neuron *10*, 21–30.

Parsons, T.D., Coorsen, J.R., Horstmann, H., and Almers, W. (1995). Docked granules, the exocytic burst, and the need for ATP hydrolysis in endocrine cells. Neuron *15*, 1085–1096.

Patterson, G.H., Knobel, S.M., Sharif, W.D., Kain, S.R., and Piston, D.W. (1997). Use of the green fluorescent protein and its mutants in quantitative fluorescence microscopy. Biophys. J. *73*, 2782–2790.

Pouli, A.E., Emmanouilidou, E., Zhao, C., Wasmeier, C., Hutton, J.C., and Rutter, G.A. (1998). Secretory-granule dynamics visualized

in vivo with a phogrin-green fluorescent protein chimaera. Biochem. J. *333*, 193–199.

Robinson, L.J., and Martin, T.F.J. (1998). Docking and fusion in neurosecretion. Curr. Opin. Cell Biol. *10*, 483–492.

Rodionov, V., Hope, A., Svitkina, T., and Borisy, G. (1998). Functional coordination of microtubule-based and actin-based motility in melanophores. Curr. Biol. *8*, 165–168.

Rogers, S., and Gelfand, V. (1998). Myosin cooperates with microtubule motors during organelle transport in melanophores. Curr. Biol. *8*, 161–164.

Saraste, J., and Svensson, K. (1991). Distribution of the intermediate elements operating in ER to Golgi transport. J. Cell Sci. *100*, 415–430.

Tooze, S., Flatmark, T., Tooze, J., and Huttner, W.B. (1991). Characterization of the immature secretory granule, an intermediate in granule biogenesis. J. Cell Biol. *115*, 1491–1503.

Trifaró, J.-M., and Vitale, M.L. (1993). Cytoskeleton dynamics during neurotransmitter release. Trends Neurobiol. Sci. *16*, 466–472.

Urbé, S., Page, L.J., and Tooze, S.A. (1998). Homotypic fusion of immature secretory granules during maturation in a cell-free assay. J. Cell Biol. *143*, 1831–1844.

Wacker, I., Kaether, C., Krömer, A., Migala, A., Almers, W., and Gerdes, H.-H. (1997). Microtubule-dependent transport of secretory vesicles visualized in real time with a GFP-tagged secretory protein. J. Cell Sci. *110*, 1453–1463.

Wu, X., Bowers, B., Rao, K., Wei, Q., and Hammer III, J.A. (1998). Visualization of melanosome dynamics within wild-type and dilute melanocytes suggests a paradigm for myosin V function in vivo. J. Cell Biol. *143*, 1899–1918.

Xu, H., and Shields, D. (1994). Prosomatostatin processing in permeabilized cells. J. Biol. Chem. *269*, 22875–22881.